Impinging Flame and Wall Interactions Studies by Using Thermal Image Camera

Abulkasim A. Asgyer[*], and Salem A. Farhat[**]

* L*ibyan Academy for postgraduate studies. (l.A.P.S). Tripoli, Libya (abulkasim.asgyer @academy.edu.ly)*
*** Department Mechanical and Industrial Engineering, Faculty of Engineering, University of Tripoli, Tripoli, Libya (salemfarhat_t@yahoo.co.ik)*

Abstract

The experimental work involves calculation of radial distribution of heat transfer flux at the surface of a flat steel un-cooled plate being impinged by a turbulent flame jet. A high temperature heat flux thermal Image camera (AGEMA Infrared system –Thermovision&900 Series) used to measure the transient total heat flux and temperature distribution at the plate surface. Qualitative temperature measurements have been performed for four identified combustion modes using a thermal-imaging camera. Flame-impinged wall temperature measurements have been performed to understand the near wall characteristics of impinging flames. The experiments have shown that the "flame switching off" technique is a reasonably accurate method for the measurements of flame impinging plate wall temperatures and heat flux. The results show that there are many factors affect the near wall flame structure and the heat transfer. These factors include the turbulence intensity, the nozzle mean flow velocity, the flame mode, and the nozzle-to-plate separation. The large vortices, which appear in the disc flame without a TG, can enhance the combustion significantly, leading to a better heat transfer to the wall. Turbulence characteristics can modify the near wall flame structure significantly and therefore, the heat transfer pattern to the flame impinged plate will be improved.

KEYWORDS: Impinging Flame; thermal image camera; flame mode; heat transfer

Introduction

Heat loss is very important technical indicator of every heat device. There are three possibility of heat transfer. The first is conduction, the second is convection and third is radiation. Heat transfer between surface of heat device and environment is evoke only heat transfer due to convection and radiation [1]. Flame or hot gas impinging for heating and material processing is widely applied in industry. In this sense, flame and wall interactions are of great real practical interests despite the fact that they are not widely investigated by the combustion communities. Unwanted impinging flames may also be encountered frequently. For instance, a pressurised fuel pipe may rupture in chemical factory and the escaping fuel jet may impinge on a near–by fuel storage tank or important structural component. If the fuel jet is accidentally ignited, the subsequently formed impinging flame could have disastrous consequences. Therefore, the wall temperature and heat flux through a flame or hot gas impinged object is always a real interest to a designer or a fire safety officer. In practice, it is very difficult to measure near–wall flow and wall temperature even under a cold flow conditions. Thermocouples are often used to measure the wall temperature but only discrete point information is available. In addition, in some cases, the surface is completely inaccessible for any direct instrumentation. At high temperature, radiation effects become significant and the calibration of thermocouple becomes

difficult. The thermal contact between a thermocouple and the wall may not be a trivial issue if impinged by flame or hot gas.

Thermal imaging camera is widely used to measure wall temperature surrounded by low emission and absorption medium such as ambient air. For reacting flow or hot gases covered wall, the thermal radiation from the wall is often masked by hot gas or flame, which makes it difficult for a thermal camera to look through. Filters might be applied to block the gaseous radiation at discrete spectra. However, the effect is often not ideal. In this study, a simple and effective method is applied to measure the wall temperature and heat flux of flame covered wall. The objectives of this study are to measure the temperature patterns of a flame-impinged wall under a various combusting modes and particular interest is focused on the disc, ring, and cone flames, as shown in Figure 1. By analysing the temperature pattern (thermal footprint) on the wall of impinging turbulent premixed flames under various combustion modes much information of local near wall flow characteristics can be obtained.

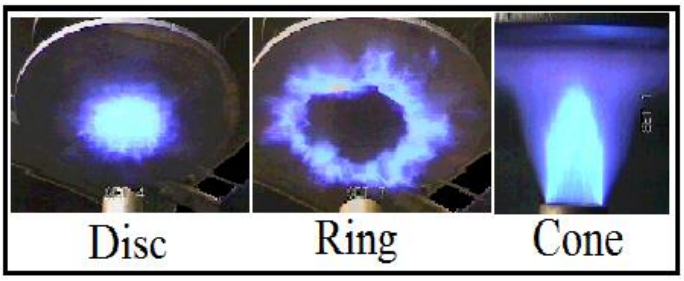

Fig. 1 Impinging flames patterns.

The AGMA Infrared System

The AGEMA Infrared system (Thermovision®900 Series) is applied for the temperature measurement as shown in Figure 2. The lens of the thermal-imaging camera is at an angle of about 40^0 relative to the imaged plate surface. The distance between the plate and the camera lens is a bout 130 mm. The infrared radiation from the plate is converted into digital signals by a scanner in the camera. The radiation received consists of radiation emitted not only from the object but also from the surroundings, from the atmosphere and also from the scanner optics. All of these factors are included in the object temperature calculation. The scanner chosen is operated in the long waveband (8-12μm) of the infrared spectrum, which is a window of interest to most of the military studies and applications, since radiation absorption by the ambient air is a minimum within this window of spectrum. The thermal scanner uses a liquid nitrogen cooled mercury cadmium telluride detector. The working temperature range is between -30 ^oC and 1500 ^oC. The sensitivity at 300 ^oC is 0.080 ^oC and the over all accuracy claimed by manufacturer is about ± 1%. The framing rate is up to 30Hz but with reduced flame size. Software called IRwinOLE is then used for post processing the acquired images. When a camera is at an angle with the filmed object, image distortion has to be corrected before any quantitative analysis. Careful tests and calibrations have been carried out. It is believed that the results presented do not suffer from image distortion.

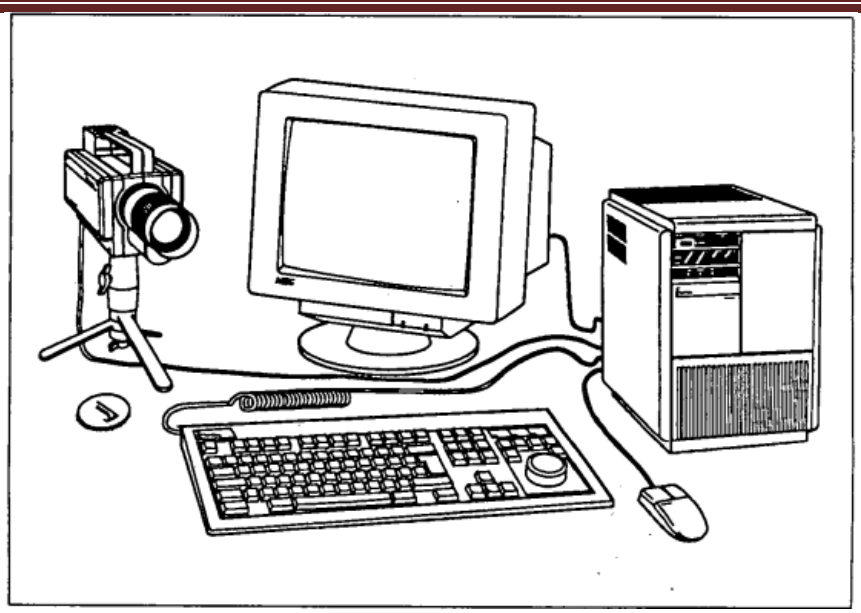

Fig. 2 The AGEMA Infrared system (Thermovision®900 Series)

Experimental Methodology

Due to the strong radiation from the impinging flame, a special method has to be applied for a thermal-imaging camera to capture the wall temperature behind the flame or hot gas product. The thermal inertial of impinged object is often high enough for a thermal imaging camera to capture the surface temperature of flame impinged plate quite accurately even though the impinging flame has been switched off temporarily. The camera used in this study is able to capture 30 images per second. If starting to capture images just before the flame switched off, the time resolution of getting a thermal image without the flame can be of order of 30 mille-seconds, which are many orders less than the thermal decay time of a flame–impinged target, which can be defined as:

$$\tau_{atm} = \frac{\rho C V}{\alpha F} \qquad (1)$$

Where: ρ is the plate density, C is the heat capacity, V/F is the volume to surface ratio and α the heat transfer coefficient.

Thermal Measurement Procedure

The plate is impinged under a particular combusting mode (e.g a disc, ring flame etc) for at least five minutes so that the temperature distribution on the plate could reach the steady state. It has been checked that the temperatures varies very little above the five minutes impinging time, chan (2000) [2]. The flame then is switched off immediately after the thermal camera has started to take images. Tests have been carried out on the repeatability of the captured temperatures by repeating the experiment under the same flow conditions at least twice on

different dates. No noticeable difference has been observed. The distortion along the centreline of the images, which is perpendicular to the lens axis, is negligible.

The temperature and heat flux profiles presented in this study are obtained only from this centreline and therefore the results will not suffer from image distortion. To extract data along any other direction, a direct calibration has to be carried out.

Heat Flux Measurement

The three basic modes of heat transfer are conduction, convection and radiation. Thermal radiation can be understood as the heat that leaves an object by way of electromagnetic radiation. Emittance is the ratio of the amount of heat radiated by a material as compared to a black body, and it is always less than one. Shiny, metallic materials tend to have low emittance, while matte, dark colored materials tend to have high emittance.

Heat transfer by radiation, is described by the Stefan-Boltzmann law[3]:

$$Q_r = \varepsilon.\sigma\left(T_{wall}^4 - T_{ambint}^4\right) \qquad (2)$$

where: Q_r is the radiation heat flow rate, ε is the emissivity of the material, σ is equal 5.67 10^{-8} [W/m^{2}K^4] (Stefan-Boltzmann constant), T_{wall} is the wall temperature [K] ,and T_{ambint} is the temperature of the surroundings [K].

Industrial infrared thermometers usually consist of different elements, such as the collecting optics, the radiation detector and some form of indicator. For the system used, the collecting optics, consisting of a germanium window and the focusing lens, are combined with a set of electromechanical servos to perform horizontal and vertical scanning, so that the whole field of view is monitored. The scan mirrors are contained in a sealed evacuated module for increased efficiency. The detector views a thermal reference target 60 times per second and the Mercury/Cadmium/Telluride detector is cooled by liquid nitrogen to 77K for maximum thermal sensitivity and spatial resolution.

Uncertainty of the Thermal Image Camera

The calibration function, which describes the scanner output as a function of blackbody temperature, is used to transform measured radiation into object temperature. The main influential parameters of the wall temperature measurement include the emissivity of the measured surface, the absorption of the atmosphere, the time response of the measured object and the ambient temperature. The first two uncertainties have been dealt with by the manufacture of the camera. The corrections for the influences of atmosphere and object emissivity can be expressed as:

$$I_m = I(T_{object})\tau_{atm}\varepsilon_m + \tau_{atm}(1-\varepsilon\ )I(T_{ambient}) + (1-\tau_{atm})I(T_{atmospheric}) \qquad (3)$$

Where I_m the thermal value for the measured radiation is, $I(T)$ represents the proportional to the emitted radiation from a blackbody radiator at temperature T, with T_{atm}, $T_{ambient}$ representing atmospheric and ambient temperatures respectively. The atmospheric transmission efficiency, τ_{atm}, is the mean atmospheric transmission between the object and the front lens for radiation within the spectral wavelength range being used. The value of τ_{atm} is calculated as a function of the object to the lens distance, the atmospheric temperature, and the relative humidity for strengthening the infrared signal.

The above equation is valid on the assumption that the surface has a constant spectral emissivity (grey body) and that the output signal of the scanner is proportional to the received radiation. In fact, the relation between the blackbody temperature and the signal output is nonlinear and a calibration function, therefore, is needed to express the non-linearity of this relation. According to the manufacturer, a calibration function in the thermal-image camera is obtained by a series of experiments yielding much more accurate results than using Plank's Law directly. The calibration function is written as:

$$I = R_f /(\exp(B/T) - F) \quad (4)$$

where T is the (greybody) temperature and, R_f, B, F are the response factor, the spectral factor, and the shape factor respectively and they are derived from experiments carried out by the manufacturer.

The compensation for the scanner temperature dependent radiation, emitted from the scanner and its optics, is performed automatically in the infrared system. A microprocessor-controlled system using two blackbody temperature references, that are scanned and four temperature sensors to measure the scanner and lens temperatures carry this out. This includes a temperature sensor, in the lens, which compensates for the radiation from the lens.

Surface Emissivity

Surface Emissivity, ε_m of the plate is one of the important uncertain factors mentioned in the previous sub-section so that careful choice of its value is an important issue to avoid a miscalculation of the emissive power of the body. According to Stefan-Boltzmann law, the total radiant emittance, W_λ, of an object with a certain ε_m, is defined as:

$$W_\lambda = \varepsilon_m \sigma T^4 \quad (5)$$

where σ is the Stefan-Boltzmann constant ($5.7\text{x}\,10^{-8}\, wm^{-2}$).

It is understood that the emissivity value of a body depends mainly on the material of the body and its surface treatments. The more realistic method is to measure its value at the ambient temperature. However, the calibration that has been already carried out by the manufacturer of

the camera is based on the emissivity at room temperature so that the temperature dependency is avoided. In this study, the emissivity calibration of the steel plate has been carried out at different temperature, the emissivity value was chosen to be 0.91 for steel plate.

Time Response of the Measured Object

The time response of an impinged plate is depending on the thermal diffusivity of the plate and the impinging flow characteristics. Figure 3 shows the impinging plate and burning system.

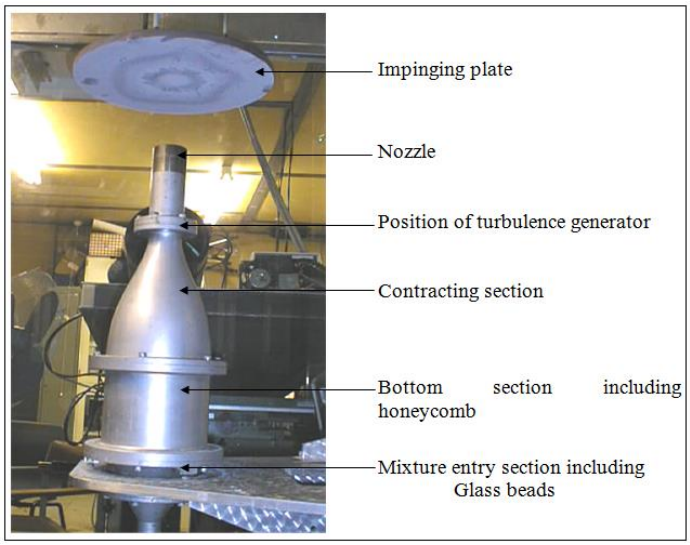

Fig. 3 impinging plate and burning system.

The former is dependent on the physical property of the plate material as shown in table 1.

Table 1 The impinged plate specifications

Material	Steel
Diameter (m)	0.3
Thickness (m)	0.01
Density (kg/m^3)	7750
Emissivity	0.91
Specific heat ($Jkg^{-1}{}^{\circ}C^{-1}$)	450
Thermal conductivity ($Jkg^{-1}{}^{\circ}C^{-1}$)	36.7 (20 $^{\circ}C$)

The working temperature range is between –30 ºC and +1,500 ºC. The sensitivity at 30 ºC is 0.08 ºC and the overall accuracy is around ± 1 % according to the manufacturer. The framing frequency is up to 30 Hz but with reduced frame size, (AGEMA Infrared System Manual).

The thermal imaging camera was operated at one frame per second. Experiments showed that there is no much difference in plate temperature during a time interval of 5 seconds, which means that the first thermal image taken after the fuel switched off can be considered as the plate temperature directly under the flame, (Chan 1999)[4].

Results and Discussions

The flame impinged wall temperature is an important factor for the understanding of the near wall flow characteristic. Experimental evidence has shown that three alternative stable combustion modes (ring, disc, and cone flames) can be established under the same nozzle exit flow conditions. The objective of the study is to investigate near-wall flow characteristics of the three different modes. To achieve this, impinged wall temperature patterns are measured and analysed. It can be seen later that the combined information of the thermography and flow structures using LDA of flames provide valuable physical insight into localised combustion chrematistics and heat transfer. The footprint of the different flame modes test cases are presented in paper [5].

Figure 4 shows the radial profiles of the normalised impinging surface temperature of disc flame, cone flame and ring flame. The profiles represent the temperature distributions from the stagnation point (r/D=0.0) radially to a radius of three nozzle diameters (r/D=3.0). All flames are created under the same nozzle exit flow conditions, nozzle to plate distance and with a TG installed. The temperature differences between the disc flame and the cone flame is around 300 ^{o}C at the stagnation point. The highest wall temperature is 865.14K and it is found at the stagnation point where the flame tip of cone flame impinges upon. If one moves radially along the plate surface away from the stagnation zone, one might see that the heat transfer of the cone flame is steady until r/D=2.5 where a noticeable small increase of the surface temperatures is found.

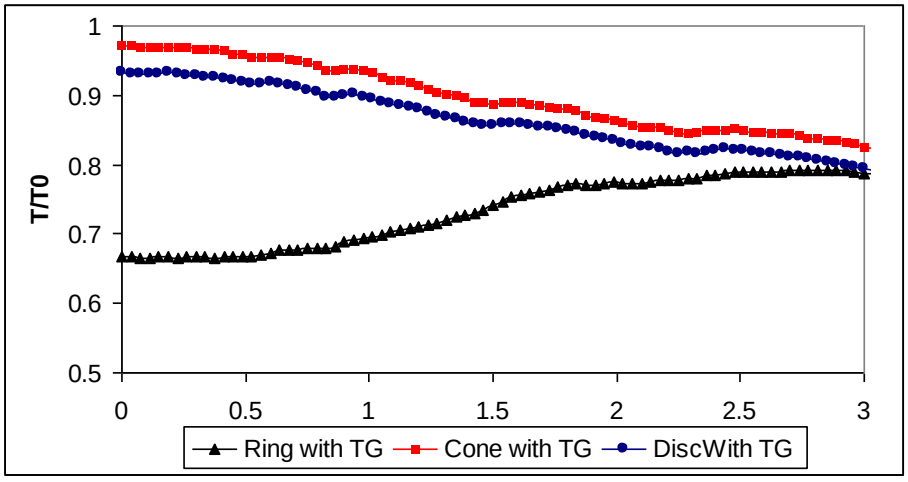

Fig. 4 Radial profiles of normalised plate temperature with a TG, Re=11300, ϕ =1.53, H/D=1.0, and T_0=865 K.

The significantly lower plate temperature in the case of ring flame mode, compared with the other two modes, suggesting that reactant may have been over diluted by the ambient air or escaped without burning. The maximum temperature of the ring flame at stagnation point is 577.12K.

Turbulence Characteristics

To investigate the effect of the turbulence intensity on characteristics of an impinging flame and its corresponding effects on heat transfer, a second set of experiments is made. Measurements are taken under the same flow conditions; however there is no turbulence generator TG installed inside the burner nozzle. According to the LDA measurement in paper [5] the turbulence intensity at the nozzle exit is reduced by 40% if the TG is not installed.

Figure 5 illustrates the impinged surface temperature profiles of the disc flame with and without a TG installed. The plate temperature around the stagnation region is generally higher in the case of flame without a TG installed, due to the generation of high vortex in the case of disc without TG and also it might be due to the high air /fuel ratio ϕ which are about 1.53 in this case. The temperature distribution for both flames is relatively flat and uniform to the plate radius r/D=1.0. Note that the temperature distribution within this region is similar despite the difference in fuel to air ratio. A noticeable increases in temperature occurs at around r/D=1.5 where it's the outer edge of the flame. In the case of disc flame without a TG it is worth mentioning that loud noise is generated.

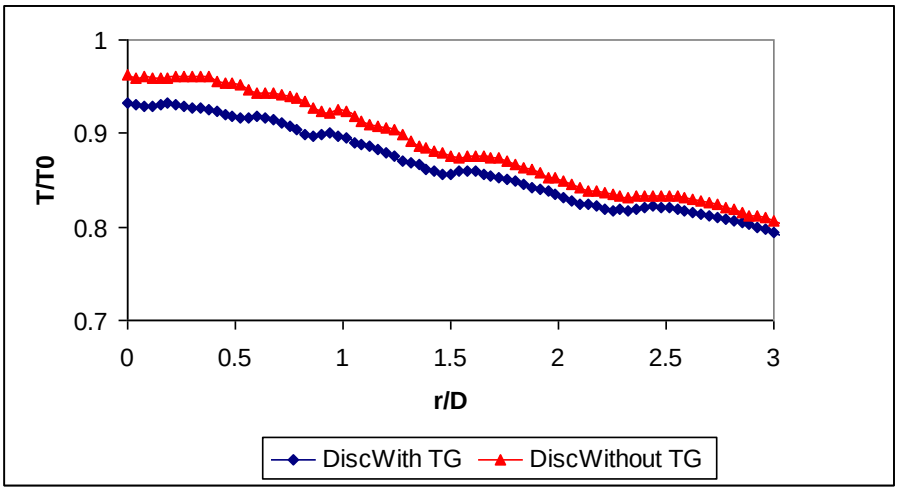

Fig. 5 Radial profiles of normalised plate temperature of the disc flame with and without a TG, Re=11300, ϕ =1.53, H/D=1.0, and T_0=865 K.

The loud noise is due to the vortex shedding and large eddy break-up around the edge of the flame. Chan and Zhang (1999) [4] in their study of sound emissions of flames argued that coherent structures are developed in the jet boundary layer, causing the tendency of inducing combustion instability at the flame edge.

Figure 6 shows the plate surface temperature profiles of the disc flame with and without a TG installed at ϕ =1.0. The temperature at the stagnation point for both flame with and without a TG found to be lower compared to the case of ϕ =1.53. As the fuel rich flames tend to have higher plate temperatures in the post flame zone r/D $\geq$ 1.5 . In addition away from the stagnation point the disc flame with TG installed have a higher temperature than that of former one, and that is due to the effect of reducing the equivalence ratio close to stoichiometry.

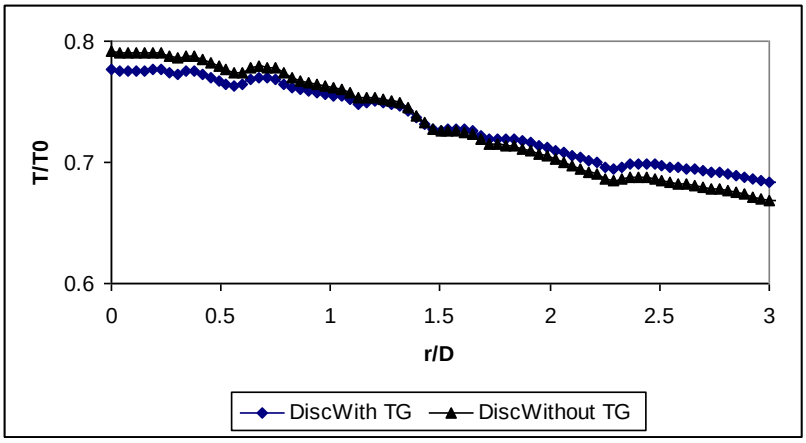

Fig. 6 Radial profiles of normalised plate temperature of the disc flame with and without a TG, Re=11085, ϕ =1.02, H/D=1.0, and T_0=865 K.

Figures 7 and 8 present the temperature profiles of the disc flames at two different Reynolds numbers, Re=11300 and Re=11085 and different equivalence ratio of ϕ =1.53 and 1 respectively. At high Reynolds number (11300) high temperature are observed in the case of disc flame without TG installed. Also intense combustion region located at $0 \le r/D \le 1.5$ where the maximum temperature is found at a stagnation point for both flames with and without a TG installed. As mentioned early, the higher temperature in the case of disc flame without a TG installed may attributed to the large vortex structure observed in the flame. The subsequent break up of the vortex may induce combustion instabilities and hence the turbulent transport and mixing process. Figure 8 shows that the disc flame with a TG installed has a higher temperature profile along the plate than that of flame without a TG and that is due to the effect of low equivalence ratio $\phi \approx 1$ and also slightly low Reynolds number. Also low temperature is observed in this case compared to Figure 8.

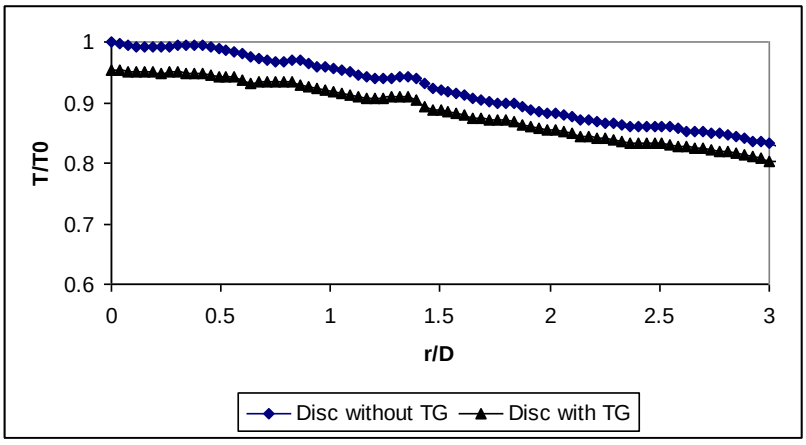

Fig. 7 Radial profiles of normalised plate temperature of the disc flame with and without a TG, Re=11300, ϕ =1.53, H/D=1.5 and T_0=847 K.

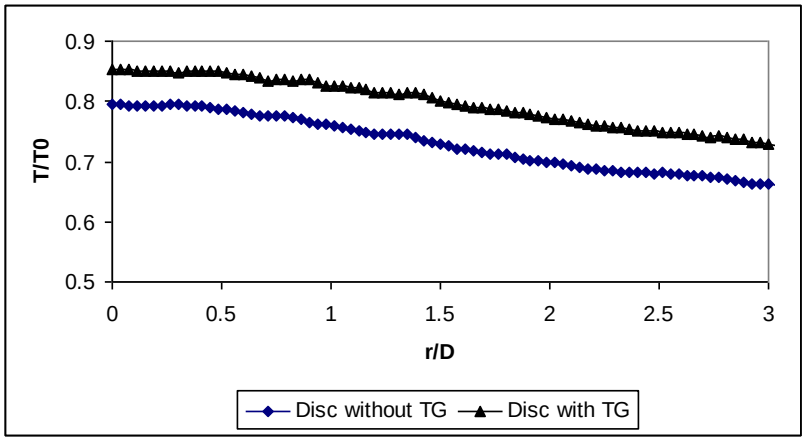

Fig. 8 Radial profiles of normalised plate temperature of the disc flame with and without a TG, Re=11085, ϕ =1.0, H/D=1.5 and T_0=847 K.

Figures 9 and 10 present the temperature profiles of the disc flames at two different Reynolds numbers of Re=9177 and Re=11195 and two different equivalence ratio of ϕ =1 and 1.27 respectively. Figure 9 large vortex structure observed in the flame without a TG installed hence high temperature are observed than that of flame with a TG installed. The subsequent break up of the vortex may induce combustion instabilities and hence the turbulent transport and mixing process. At higher Reynolds number of 11195 high temperatures is observed in the case of disc flame with a TG installed. Also intense combustion region located between $0 \le r/D \le 1.5$ where the maximum temperature is found at a stagnation point for both flames with and without a TG installed. As mentioned early, the higher temperature in the case of disc flame with a TG installed in this case may attribute to the change in equivalence ratio. In this case we can conclude that the flame is so sensitivity to the change in equivalence ratio.

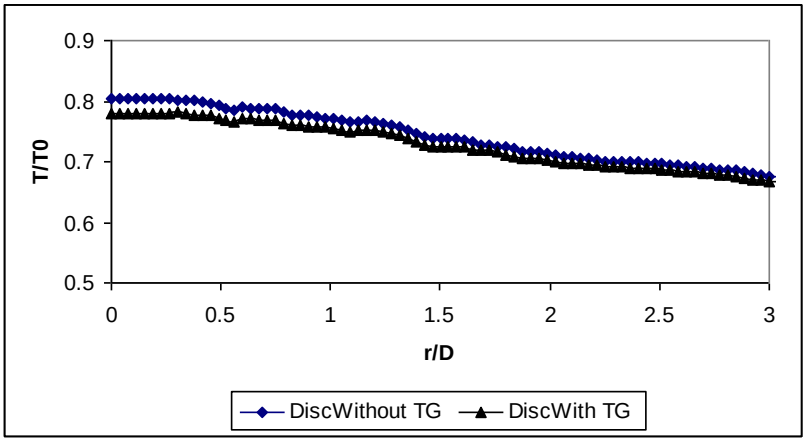

Fig. 9 Radial profiles of normalised plate temperature of the disc flame with and without a TG, Re=9177, ϕ =1.02, H/D=1.0 and T_0=865 K.

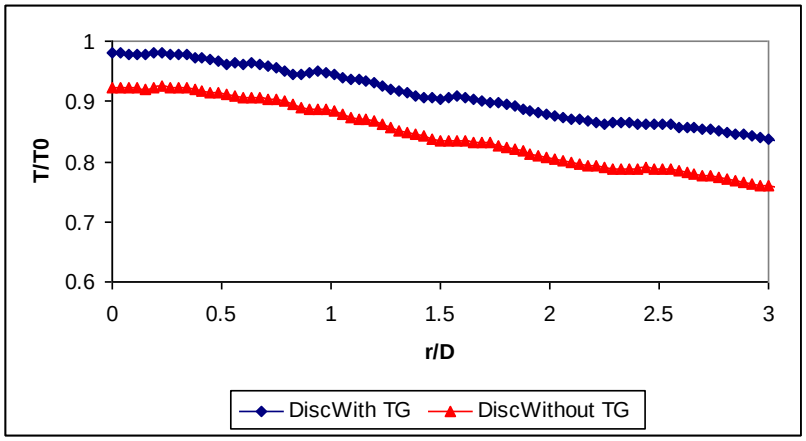

Fig. 10 Radial profiles of normalised plate temperature of the disc flame with and without a TG, Re=11195, ϕ =1.27 H/D=1.0 and T0=865 K.

Figure 10 shows that the disc flame with a TG installed has a higher temperature profile along the plate than that of flame without a TG and that is due to the low equivalence ratio $\phi \approx 1.27$ and also slightly higher Reynolds number.

Also from the figures we can observe strong heat transfer from the gas to the plate.

Figure 11 compares two cone flames with and without a TG installed at the same flow conditions. This figure indicates that turbulence has a very strong influence on the flame structure and the consequent heat transfer process to the impinged plate. Without a TG installed, cone flame gives higher surface temperatures throughout the plate. The combustion of the cone flame with and without a TG occurs in a very thin shear layer all the way up from the nozzle exit to the impinging plate. There is no combustion in the potential core region.. Also higher temperature is observed for the cone flame without the TG installed. Higher temperatures are also observed at r/D=2.5. The heat transfer in this region is influenced by the presence of the flame.

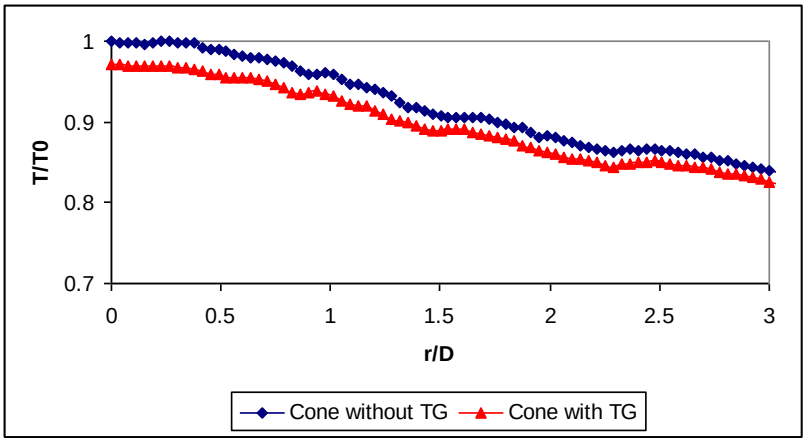

Fig. 11 Radial profiles of normalised plate temperature of the cone flame with and without a TG, Re=11300, ϕ =1.53, H/D=1.0 and T0=865 K.

Ring flames with and without a TG installed are investigated. Figure 11 shows the both flames at the same flow conditions (ϕ =1.53, H/D=1.0, Re=11300). As mentioned in paper [1] of impinging flames patterns, ring flames are plate stabilised flames. There is no combustion in the stagnation zone and, hence the centre part of the plate is relatively cool. Combustion, therefore, occurs only at a position where the radial wall jet velocity (radial velocity) is reduced to an appropriate level. For more information see paper [6].

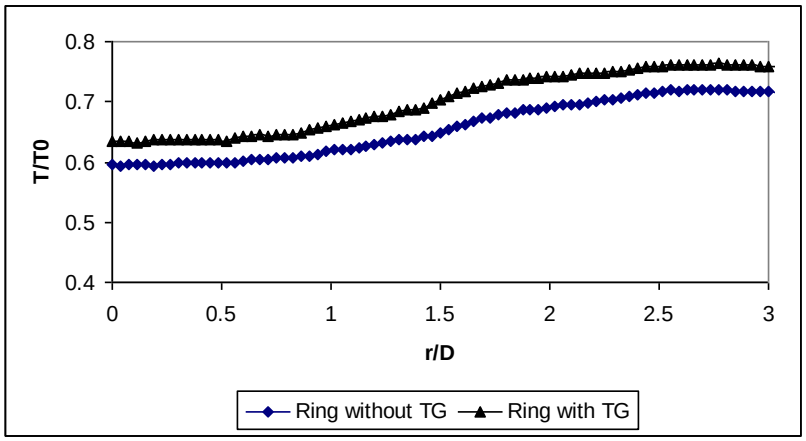

Fig. 12 Radial profiles of normalised plate temperature of the ring flame with and without a TG, Re=11300, ϕ =1.53, H/D=1.0 and T_0=865 K.

Surprising result can be seen in Figure 12 comparing to the other modes at the same flow conditions. The ring flame with a TG installed gives higher impinging temperature than that of flame without a TG installed. This indicates that the flame with a TG has more mixing and more complete combustion occurs.

Figure 13 illustrates the normalised radial profiles of plate surface temperature of four tested disc flames, with and without a TG installed and at different H/D, (H/D=1.0 and 3.0). As we can see from the figure in the case of H/D=1.0, both flames with and without a TG give very similar impinged surface temperatures outside the stagnation zone and as mentioned early higher temperature for the flame without a TG installed due to the high vortex hence more mixing and complete combustion. Figure 12 also indicates that the stagnation temperature would increase with H/D. Both disc flames in the case of H/D=3.0 clearly produce higher impinging temperature in the stagnation region, suggesting that much of the combustion reactant cloud not burn adequately in the case of H/D=1.0, due to the flow developed. Comparing the flames with and without a TG in the case of H/D=3.0, flame with the TG installed gives higher temperature profile, particularly in the stagnation zone.

Radiation heat flux from the flame impinged plate

Heat balance of the plate is achieved by convection, conduction and radiation. This section focuses on the radiation heat transfer from the impinged plate in a various flame modes. The total heat transfer from the hot gases to the impinged plate can be balanced by radiation losses

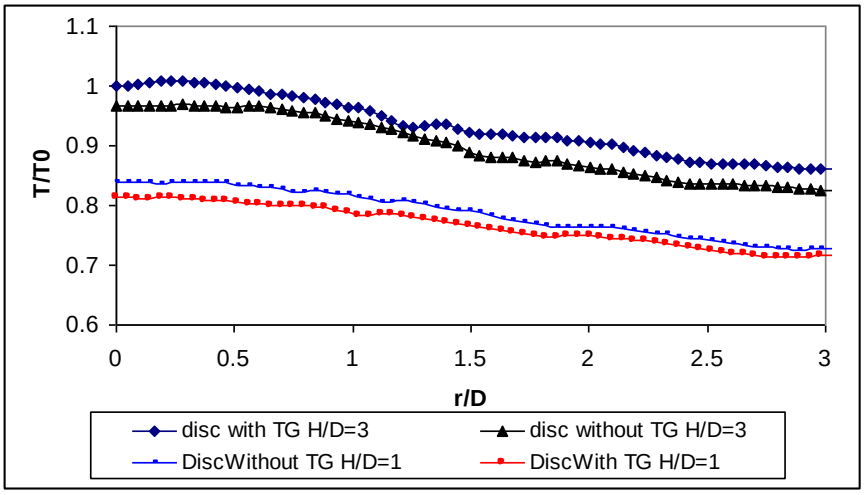

Fig. 13 Radial profiles of normalised plate temperature of the disc flames with and without TG, at Re=11300, ϕ =1.53 when H/D=1.0, 3.0 and T_0=865 K.

from the impinged and the rear surfaces, plus the natural heat convection from the rear surface. For the steel plate the heat conductivity is quite high. The temperature difference between the two surfaces will be relatively low Chan. (2000)[2]. Therefore, estimated radiation heat flux from the rear surface of the plate will be the same order as the flame impinged side. The radiation heat from the flame impinged plate can be estimated by:

$$q''_{rad} = \varepsilon\sigma\left(T_w^4 - T_a^4\right) \text{ W/m}^2 \qquad (6)$$

where ε is the emissivity of the plate $(\varepsilon = 0.91)$ for the oxidised steel plate(assumed).,

σ is the Stefan-Boltmann constant, T_w is the impinging plate temperature in Kelvin and T_a the ambient temperature.

Figure 14 shows the normalised profiles of the radiation heat flux along the plate. The value of the $q''_{0.rad}$ is taken as approximately 38.8 KWm^{-2}. The figure indicates that the disc flame with a TG shows a stronger variation of heat transfer in the stagnation region and also along the wall impinged region. The disc flame without a TG almost has a constant heat flux in the stagnation region. Figure 15 shows the profiles of the heat flux of the disc flames without a TG installed at ϕ =1.53. High temperature peaks caused by the strong flame vortices becomes very obvious as H/D increases. Also the heat flux variations are higher as the H/D increases. The flame noise in the case of H/D=3.0 is higher than the cases of H/D=1.5, and H/D=1.0. Variation of the radiation heat flux of the ring flames with and without a TG at ϕ =1.53 and H/D=3.0 is given in Figure 16. The radiation heat flux for the ring flame with a TG is much higher than that of ring flame without a TG. This figure also shows that the heat flux for both cases is constant along the plate. The comparison of radiation heat flux of the ring flames, with a TG and at different values of H/D (3.0, 1.5 and 1) are shown in Figure 16. The radiation heat flux increases with the increase of H/D, and there is a significant increase of heat flux in the case of

H/D=3. Comparing with the radiation heat flux of the disc flames the heat flux patterns are much simpler.

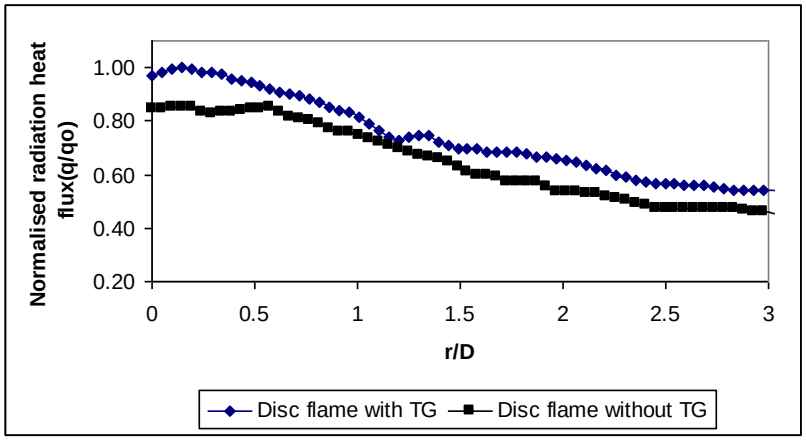

Fig. 14 Normalised radiation heat flux of the plate impinged by disc flames with and without a TG, at ϕ =1.53, H/D=3.0, and q_0 =38.8 kWm^{-2}.

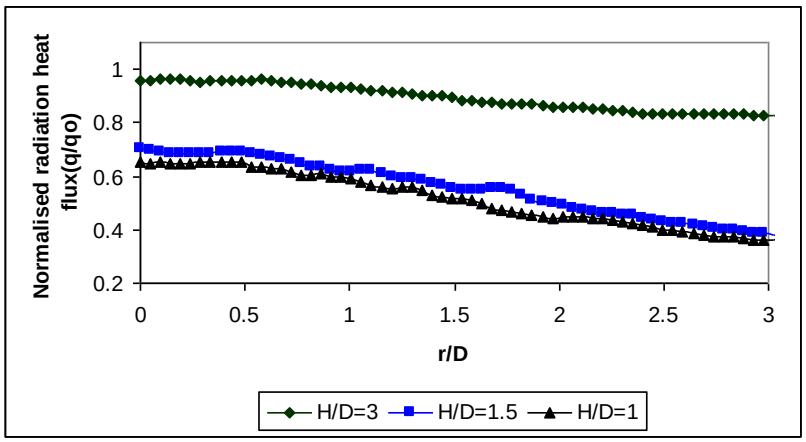

Fig. 15 Normalised radiation heat flux of the plate impinged by disc flames without a TG, at ϕ =1.53, and q_0 =38.8 kWm^{-2}.

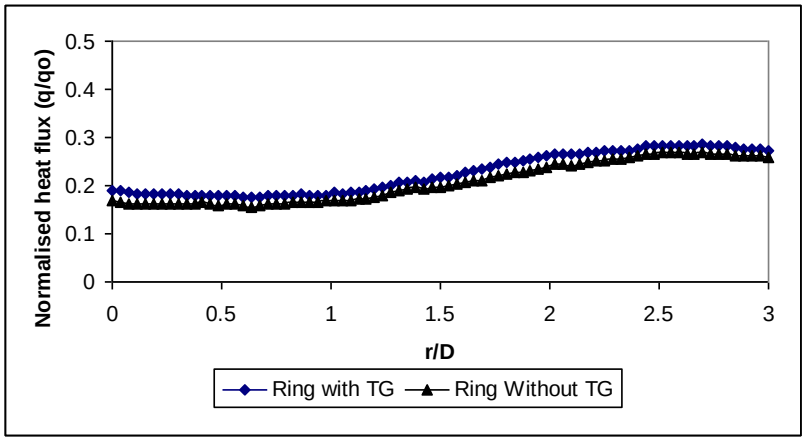

Fig. 16 Normalised radiation heat flux of the plate impinged by ring flames with and without a TG, ϕ =1.53, H/D=1.5, and q_0 =27.35 kWm^{-2}.

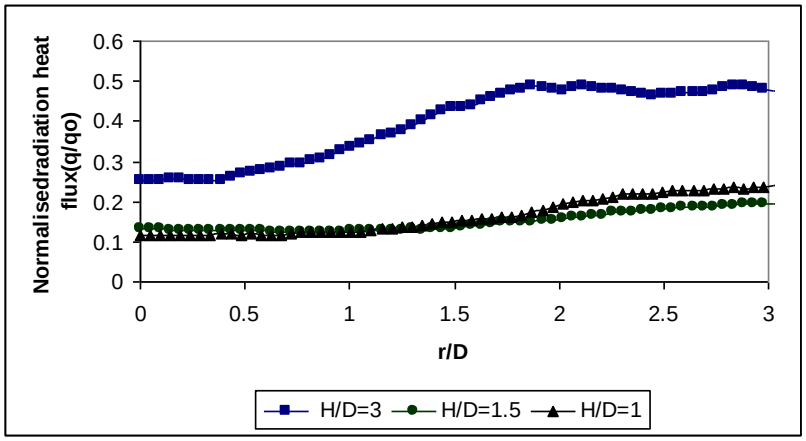

Fig. 17 Normalised radiation heat flux of the plate impinged by ring flames with a TG, ϕ =1.53, and q_0 =38.8.35 kWm^{-2}.

Normalised profiles of the radiation heat flux of the cone flames with and without a TG installed at $\phi = 1.53$ and H/D=1.0 are shown in Figure 18. From the figure, one can see that the flame without a TG installed have higher heat flux than that with a TG. The heat fluxes are almost the same in the wall jet region for the flames with and without a TG installed. Figure 19 shows the radiation heat flux of the cone flames with a TG and at different values of H/D. Higher heat flux is observed in the case of low H/D in the stagnation region. In the wall jet region one can notice that the heat radiation flux of H/D=3.0 is higher.

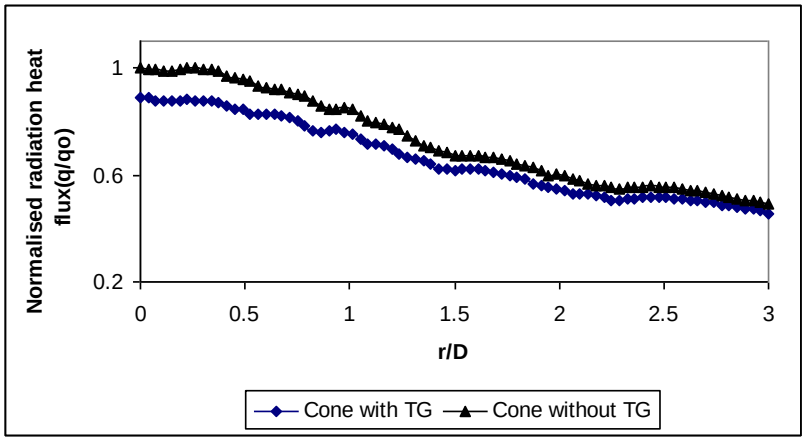

Fig.18 Normalised radiation heat flux of the plate impinged by cone flames with and without a TG, ϕ =1.53, H/D=1.0, and q_0 = 29.8 kWm^{-2}.

Conclusions

To study the temperature patterns of turbulent premixed impinging flames, thermal-imaging technique has been used. The experimental results in this chapter have demonstrated that a thermal imaging camera can be a powerful and effective tool for studying the flame and wall interactions, if the camera is properly calibrated and the thermograms are processed by

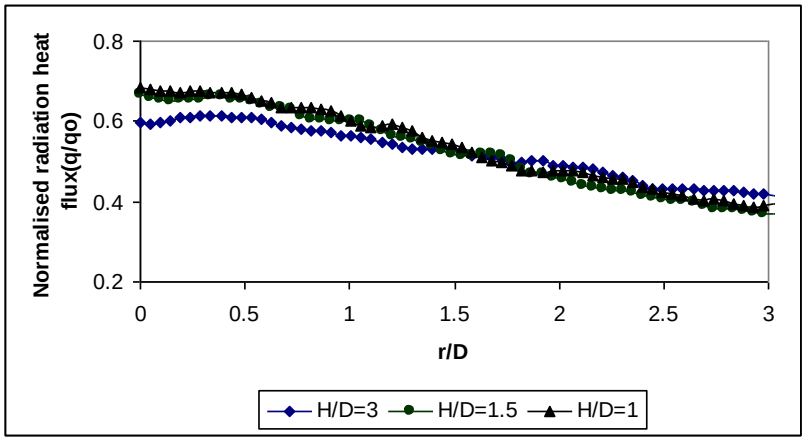

Fig. 19 Normalised radiation heat flux of the plate impinged by cone flames with a TG, ϕ =1.53, and q_0 = 38.8.35 kWm^{-2}.

appropriate software, very useful quantitative results can be obtained. The experiments have shows that the "flame switching off" technique is a reasonably accurate method for the measurements of plate temperatures and heat flux. By analysing the plate temperature patterns obtained from the footprints of the impinging reacting jets, the flow characteristics near the impingement surface under various combusting modes are investigated. The results show that there are many factors affecting the near wall flame structure and the heat transfer. The identified factors are the turbulence intensity, the nozzle mean flow velocity, the flame mode, the nozzle-to-plate separation and the air to fuel equivalence ratio. The large vortices, which appeared in the disc flame without a TG, can enhance the combustion significantly, leading to a better heat transfer to the wall. Turbulence characteristics can modify the near wall flame structure significantly and hence the heat transfer pattern to the flame impinged plate.

References

[1] Vítěz, P. Trávníček "THE MEASUREMENT OF HEAT LOSS WITHUSE OF A THERMAL IMAGING SYSTEM" Acta Universitatis Agriculturae et Silviculturae Mendelianae Brunensis 59(3):193-196 (2011)

[2] Chan. W.T., PhD Thesis, Modelling and Measurements of Turbulent Flames, ***UMIST,*** (2000).

[3] YUNUS A. CENGEL, "HEAT TRANSFER" second edition. Book.

[4] Chan, W.T., and Zhang, Y., Measurement of Flame covered Wall temperature and a Detour Visualisation of Near Wall Flow characteristics, *Joint Meeting of the British, German and French Sections, Nancy, France*, pp. 351-353 (1999I)

[5] Zhang, Y., Bary, K.N.C., Characterization of Impinging Jet Flames, *Combustion and Flame*, vol. 116: 671-674 (1999).

[6] Ali Abulkasem and Zhang. Y., The LDA Measurements of Flow Characteristics of Turbulent Premixed Impinging Flame, *2nd International conference on Heat Transfer, Fluid Mechanics and Thermodynamics*, Zambia (2003).